Strategies to Develop Highly Reactive Red Photoresists via Modulation of the Exposure and Developing Processes

*Ji Li[1, 2, 3], Hao Fang[3], Xia Zhang[3], Xiao Liu[3], and Hong Meng[1, 2]**

[1] School of Materials Science and Engineering, Peking University, Beijing 100871, China
[2] School of Advanced Materials, Shenzhen Graduate School, Peking University, Shenzhen, Guangdong, 518055, China
[3] TCL China Star Optoelectronics Technology Co., Ltd, Shenzhen, Guangdong, 518132, China

Abstract

This study focuses on improving the manufacturing efficiency of thin-film transistor liquid crystal displays (TFT-LCD) by developing color photoresists (CPRs) with higher reactivity and faster photocuring. It was found that adjusting the composition of photoinitiators, resins, and monomers led to a fast-curing red photoresist with high sensitivity. The study explored the effects of composition on pattern integrity, linewidth, and film thickness. By optimizing the ratio of these components, complete photocuring was achieved at an exposure energy of 30 mJ, maintaining target linewidth and minimizing undercut (approximately 0.6 μm). This approach balances photocuring and development properties, providing a strategy for creating highly reactive CPRs and guiding future photoresist development.

Author Keywords

TFT-LCD; Red photoresist; Photolithography; Photocuring; Sensitivity

1. Introduction

During the rapid iteration of display technology, TFT-LCD has become the mainstream product due to its advantages of low cost, high resolution, low power consumption and long service life [1-3]. TFT-LCD utilizes the optical characteristics of liquid crystals under different voltages to control the brightness and realizes the colorful display by mixing different colors through color filters (CFs). CFs are usually composed of three basic primary colors, including red, green and blue, and play a decisive role in the brightness (transmittance), contrast ratio and color saturation [4]. CFs are produced by multiple-step lithography of CPRs, including coating, drying, exposure, development, and baking (Figure 1) [5]. The exposure process is the most critical procedure of the entire lithography, which directly affects the shape, resolution, adhesion, linewidth and other characteristics of CF patterns. In addition, the efficiency of the exposure process significantly affects the production rhythm of CFs. When the power of the exposure machine is 33 mW/cm^2, the curing time is 1.33 seconds for 40 mJ exposure does, and 0.91 seconds for 30 mJ exposure does. Therefore, to further shorten the production time and improve the production capacity, TFT-LCD panel factory requires more reactive CPRs which can be rapidly cured in a shorter period.

CPRs are formulated materials with multiple components, mainly composed of pigments (or dyes), resins, reactive monomers, photoinitiators, solvents and additives [6, 7]. During the exposure process, the photoinitiator absorbs light of certain wavelengths and transitions from the ground state to the excited state. The photoinitiator then generates free radicals and initiates cross-linking reactions of multi-functional reactive monomers (or oligomers), causing substantial changes in solubility [8]. Therefore, photoinitiators, resins and monomers are important components that determine the photocuring properties of CPRs. Huang et al. prepared three transparent photoresists using three different commercial photoinitiators, Irgacure 369, Irgacure 907 and Irgacure OXE-02, and compared the rate of film residues after development at different exposure energies [9]. Among them, Irgacure OXE-02 had the highest ratio of film residues after development at the same exposure energy, which was due to the widest UV absorption peak. The results suggested that this class of photoinitiators could achieve sufficient crosslinking at even low exposure energy. Dietliker et al. applied α-aminoacetophenone, trichloromethyltriazine and oxime ester to three CPRs of red, green and blue colors [10]. They found that in blue PR, trichloromethyltriazine-derived initiators could effectively reduce the UV absorption interference of blue pigments due to the red-shift absorption peak. Therefore, a higher sensitivity could be achieved by trichloromethyltriazine rather than the other two initiators, indicating that a lower energy dose was required to achieve an intact pattern. In green and red CPRs, oxime ester displayed higher sensitivity due to less absorption interference from pigments. Sameshima et al. from BASF developed a series of oxime ester photoinitiators and found that the introduction of benzotriazole could not only improve the absorption intensity at the i-line (360nm), but also improve the quantum efficiency of its photolysis reaction through UPLC [11]. Combining the two advantages, efficient bottom-curing was achieved, and thus these kinds of photoinitiators could be applied to black or blue photoresists whose bottom layers were difficult to cure.

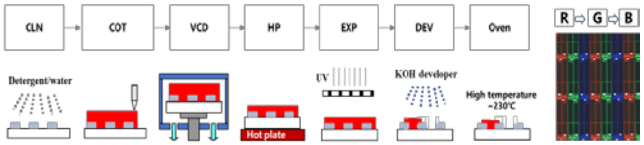

Figure 1. State transition diagram of cholesteric liquid crystal. Schematic diagram of lithography process of CF films. This process consists of the following steps: a) Cleaning (CLN): The glass substrate is cleaned thoroughly. b) Coating (COT): Application of photoresist to form a film on the substrate. c) Vacuum Cooling Dryer (VCD): Using a vacuum cooling dryer to ensure complete drying of the photoresist film. d) HP: The coated substrate undergoes an initial pre-baking step to remove some solvents from the film. e) EXP: Utilizing an exposure machine for precise exposure of the substrate. f) DEV: Following exposure, the developing process is carried out to create the desired pattern. g) Oven: Finally, the prepared pattern undergoes a curing process in an oven.

The research mentioned previously was mainly carried out on photoinitiators. Nevertheless, monomers, resins and photoinitiators are all significant components in photochemical reactions. Together, they affect the sensitivity of CPRs. In addition, the modification of the sensitivity will cause changes in critical characteristics of CRRs such as adhesion and linewidth, so it is necessary to adjust the development performance simultaneously

ISSN 0097-996X/25/5603-2184-$1.00 © 2025

to achieve a balance of the sensitivity and other key performance. In this paper, the photolithography process of red photoresist with different recipes was evaluated by changing the ratios and types of photoinitiator, resin and monomers. The highly reactive red photoresist which could be cured completely with exposure energy of 30 mJ was obtained. The resulting photoresist exhibited good pattern integrity and linewidth. This study can provide an alternative strategy for the recipe design and material selection of highly reactive CPRs.

2. Materials and methods

2.1. Materials

To prepare highly reactive red photoresist, oxime ester derivatives with high reaction efficiency were selected. Monomers with six functional acrylate groups and polyacrylate resins with carboxyl groups and unsaturated double bonds were utilized. Three recipes were designed to study the effect of the ratios of the photoinitiator and resin/monomers, as well as the type of monomers on the exposure and development properties (Table 1).

Table 1. Compositions of red photoresists used in this research.

Composition	Recipe 1	Recipe 2	Recipe 3
Mill bases	R254+R177+Y150		
Resin	R1		
Monomers (G6-AG-001/DPEA-12)	3.2%/2.4%	3.4%/2.5%	2.9%/3.0%
Resin/monomers	35%/65%	30%/70%	30%70%
Photoinitiator (P.I.)	0.19%	0.23%	0.23%
Solvents	PGMEA+MBA		
Additives	0.31%		

These six components listed below were chosen as the fundamental materials for red photoresists used in this paper:

a) Mill bases, including R254, R177 and Y150, were provided by SANYO COLOR WORKS.

b) The resin, R1, was purchased from RESONAC POLYMER MATERIALS CO., LTD (Scheme 1c).

c) Monomers, including G6-AG-001 and DPEA-12 (Scheme 1a and 1b).

d) The photoinitiator, P.I., oxime ester I-1, was purchased from TRONLY NEW ELECTRONIC MATERIALS CO., LTD.

e) Additives, including A1, A2 and A3, were purchased from DIC and ADEKA.

f) Solvents, including propylene glycol monomethyl ether acetate (PGMEA) and thiosalicylic acid (MBA), were purchased from MERCK and DAICEL, respectively. The solvents were used directly without further purification.

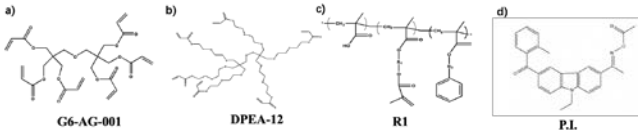

Scheme 1. Chemical structures of (a) G6-AG-001, (b) DPEA-12, (c) R1 and (d) P.I.

2.2. Experimental methods

2.2.1. The preparation of PRs

The photoinitiator, resin, reactive monomers and solvents were mixed and stirred for 30 min, followed by the addition of surfactants. The mixture was stirred for another 30 min to get a transparent liquid. The liquid was then added to the prepared mill bases and mixed for 1 hour. The resulting mixture was filtered by a 0.5 μm filter to obtain the final photoresist.

2.2.2. Photolithography conditions and equipment

Glass substrates (10 cm ×10 cm, width = 0.5mm, AGC) were cleaned by the EUV machine (SUS720, Ushio) before utilization. A photoresist layer with a thickness of 2.4 μm was then prepared with a spin coater. The substrate was let stand for 5 min and pre-baked at 90 °C for 88 s to remove solvents. Later, CPR was exposed to UV light (40 mJ and 30 mJ) to form an insoluble network. The unreacted residues were dissolved by 0.042% KOH to form patterns. Finally, post-bake was conducted at the temperature of 230 °C for 18 min to completely cure the photoresist and obtain a stable pattern.

2.3. Characterization

2.3.1. Optical microscopy (OM)

An optical microscope (OLYMPUS) was exploited to observe the contours and defects of the PR pattern and measure the width

2.3.2. Scanning electron microscopy (SEM)

A scanning electron microscope (JEOL) was used to observe the morphology of red PR after exposure and development processes.

2.3.3. Photo-induced force infra-red spectral analysis (PIF-IR)

Photo-induced force microscope (PIFM, Molecular Vista/Vista 75) was utilized to analyze the surface, middle and bottom of the red PR after exposure in situ.

2.3.4. Film thickness measurement

A α-step profiler was applied to measure the film thickness after photolithography.

2.3.5. Linewidth measurement

An optical microscope (OLYMPUS) was employed to measure the linewidth of photoresists after photolithography.

3. Results and discussion

3.1. The mechanistic analysis of material behavior during exposure and development

The reactivity of photoresists is usually characterized by photosensitivity, which refers to the minimum energy required to form an intact and stable pattern by lithography. The lower the

photosensitivity, the faster the material reacts. The red photoresist prepared by Recipe 1 was exposed to 40 mJ and 30 mJ, respectively, to obtain a pattern with 103 μm linewidth. It was discovered that the edge of the linear pattern was missing after development at the exposure energy of 30 mJ, while the pattern formed by 40 mJ exposure was clear and intact, indicating the photosensitivity of Recipe 1 was 40 mJ (Figure 2).

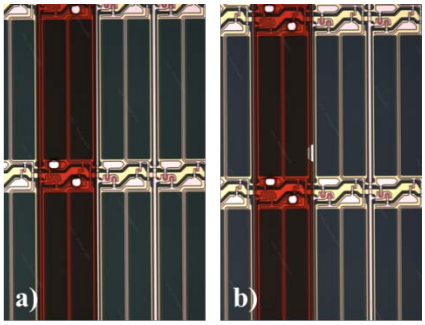

Figure 2. Microscope images of photoresist patterns after development. (a) Patterns formed by 40 mJ exposure energy. (b) Patterns formed by 30 mJ exposure energy.

To analyze the reason for the pattern peeling, the microscopic morphology formed by Recipe 1 after development and oven was observed. By comparing the SEM cross-section of the linear pattern with exposure energy of 40 mJ and 30 mJ, it was found that the bottom of the pattern after development started to hollow from the edge, showing an undercut situation (Figure 3a and 3c). Under the condition of 40 mJ exposure, the undercut depth was relatively small (0.8 μm), while the bottom exhibited a deep undercut (1.7 μm) with 30 mJ exposure. The phenomenon was speculated to be related to the insufficient crosslinking reaction at the bottom of photoresists. In the process of exposure, UV light was incident from the upper surface of the film through the material to the lower surface. According to the Lambert-Beer law, the effectiveness of UV light at the bottom was reduced significantly due to the absorption by pigments and photoinitiators in red photoresists. Therefore, the crosslinking reaction at the bottom was incomplete. In this situation, the small exposure energy resulted in insufficient bottom curing, and thus the bottom was more likely to be eroded by the developer, causing the pattern peeling. However, in the oven process, the material still displays thermal flow at a high temperature (230 °C) due to the incomplete crosslinking. Therefore, after baking at a high temperature, the bottom undercut collapsed and formed a normal pattern (Figure 3b and 3d).

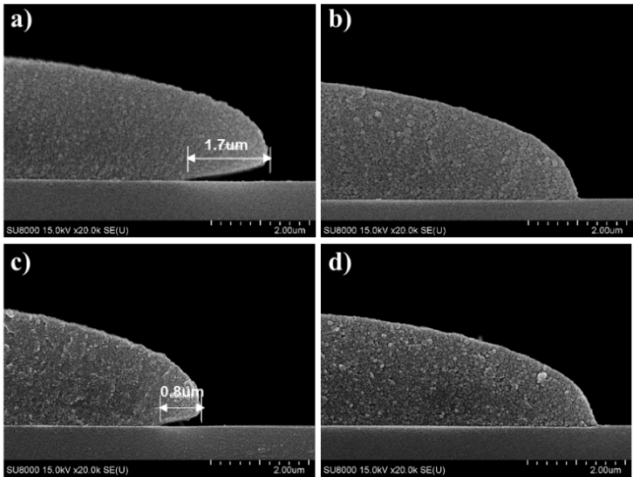

Figure 3. The SEM cross-section of the linear pattern. The cross-section (a) before and (b) after the post-baking process with 30 mJ exposure. The cross-section (c) before and (d) after the post-baking process with 40 mJ exposure.

The IR spectrum of the surface, middle and bottom layer for the Recipe 1 sample formed by 30 mJ exposure was analyzed by PiFM (Figure 4). The ratio of unsaturated C=C at 1647 cm^{-1} and C=O at 1735 cm^{-1} was used to characterize the relative polymerization degree of CPRs. It was demonstrated that the polymerization degree at the bottom of the photoresist film was relatively lower than that at the surface and the middle layer, fitting the theory that the bottom was hollowed out due to insufficient crosslinking. However, comparing the trend of the surface and the middle layer, the polymerization degree of the surface layer was not the highest. This was because the surface layer was in direct contact with air, and oxygen had a quenching effect on the free radical reaction during the exposure process, leading to an incomplete reaction.

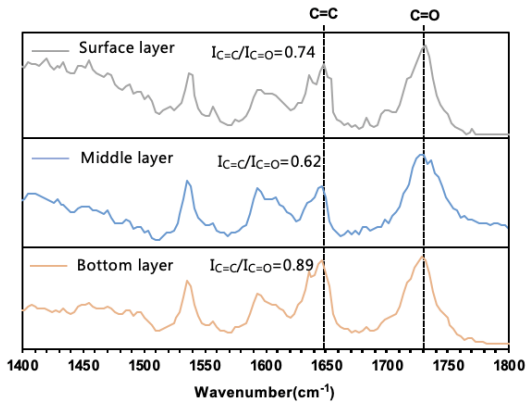

Figure 4. The PiF-IR spectrum of Recipe 1 after exposure with 30 mJ energy.

In addition to the bottom etching of CPRs, the influence of the developer on the surface layer during development was further analyzed. Because of the direct contact of the surface photoresist with the developer, incomplete crosslinking of the surface photoresist would cause the loss of film thickness by surface etching. As shown in Figure 5, when the exposure energy increased from 30 mJ to 40 mJ, the film thickness increased by about 0.15 μm. Moreover, the film thickness became relatively stable until 40 mJ. The increase in film thickness was due to more sufficient

crosslinking at higher doses and less surface erosion by the developer, proving that Recipe 1 had an insufficient reaction at 30 mJ exposure.

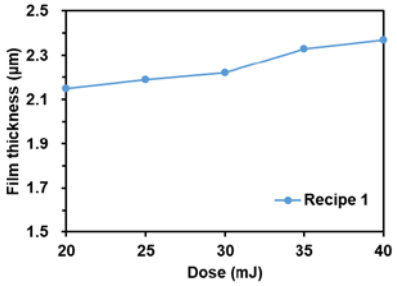

Figure 5. The relationship between exposure energy and film thickness of Recipe 1.

3.2 Design strategy of highly reactive CPRs

During the exposure-developing process of CPRs, complex chemical transformations occur. During exposure, varying reaction degrees occur at different positions due to the different environments and locations of the top, middle, and bottom layers of the photoresist. Insufficient reactions at the bottom layer are prone due to competing absorption, while surface reactions are hindered by oxygen diffusion. When it comes to the developing process, the surface and edges of the CPRs are primarily eroded by the developing solution. In this case, surface etching results in loss of film thickness and edge etching affects the critical dimensions of the CF patterns. On the other hand, the bottom reaction is, bottom erosion would also occur because of inadequate photo reaction in the bottom and thus impacts the adhesion of the CF pattern.

From the analysis in section 3.1, it is evident that achieving high reactivity hinges on ensuring sufficient reaction at the bottom of the CPRs. Among the materails of CPRs, the types and concentrations of the initiator are significant factors. The higher the initiator's absorption rate and free radical conversion efficiency under the exposure source, the higher the initiation efficiency. This study utilizes oxime ester initiators, which exhibit strong absorption at 365nm and are commonly used in the industry for their high efficiency. Increasing the content of photoinitiators, along with a suitable increase in the content of reactive monomers, increases the concentration of reactive radicals (initiator and monomer radicals) within the material during exposure. This enhances the overall system's reactivity, addressing the issues of surface and bottom erosion in color photoresist materials. However, increasing reactivity simultaneously weakens edge erosion, resulting in larger line widths of CF patterns. To address this, enhancing the developing performance of reactive monomers and strengthening the development speed at the edges during the developing process are proposed. This ultimately achieves a balance in developing across the surface, edges, and bottom of the material system, obtaining a complete CF pattern with target line widths. The schematic strategy could be found in Figure 6.

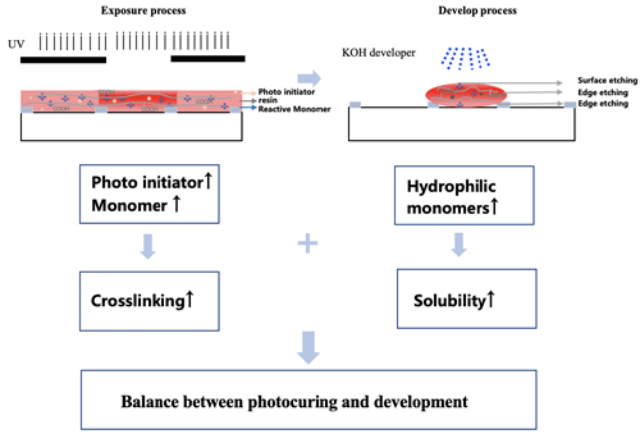

Figure 6. Schematic of modulating the exposure and developing processes to obtain highly reactive CPRs.

3.3. The optimization of material reactivity

To improve the sensitivity of the material, Recipe 2 with a higher ratio of photoinitiator and reactive monomers was designed according to the role of each component in the exposure (Table 1). The increase of the photoinitiator and monomers was conducive to free radical polymerization by increasing the concentration of free radicals. With 30 mJ exposure, the polymerization degrees of the surface, middle and bottom layers of Recipe 2 were all increased compared to Recipe 1, along with a smaller bottom undercut (Figure 7 and 8a). Therefore, the integrity of the pattern can be maintained after development without edge peeling.

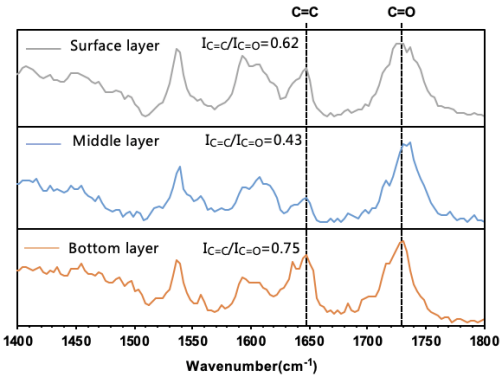

Figure 7. The PiF-IR spectrum of Recipe 2 after exposure with 30 mJ energy.

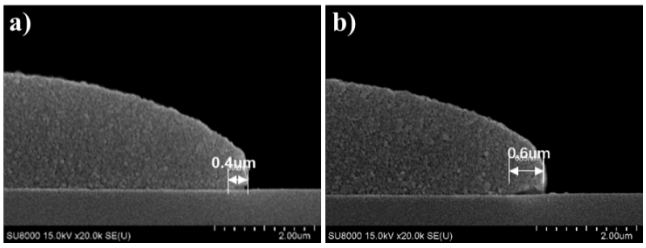

Figure 8. The SEM cross-section images after exposure. The cross-section of (a) Recipe 2 and (c) Recipe 3 after 30 mJ exposure.

The linewidth of patterns formed by Recipe 1 and Recipe 2 was then measured under OM (Table 2). Under the same manufacturing conditions, the linewidth of Recipe 2 was larger than that of Recipe 1, validating a more sufficient crosslinking of Recipe 2 than Recipe 1. In other words, under the same exposure energy, the bottom and edge of Recipe 2 could be cured more completely, resulting in larger linewidth. By comparing the dose-film thickness curves of Recipe 1 and 2, it was discovered that the film thickness of Recipe 2 tended to be stable after 30 mJ, and thus the pattern could be maintained intact under this condition (Figure 9). Therefore, the photosensitivity of Recipe 2 was at the level of 30 mJ.

Table 2. Linewidth and hole sizes of Recipe 1 and Recipe 2 after the post-baking process.

Photoresist	Recipe 1	Recipe 2
Linewidth (μm)	103.38	108.60
Hole size (μm)	18.97	18.19

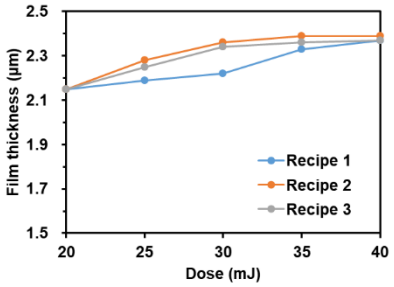

Figure 9. The relationship between exposure energy and film thickness of Recipe 1, 2 and 3.

3.4. The adjustment of the balance between photocuring and development

As mentioned previously, the adjustment of sensitivity may influence the adhesion property and linewidth of the photoresists. Therefore, the development property should be modified simultaneously along with the sensitivity. To deal with the problem of excessive linewidth of Recipe 2, Recipe 3 was designed (Table 1). By maintaining the ratio of photoinitiators and resins/monomers, increasing the amount of hydrophilic reactive monomers, DPEA-12, could enhance the solubility of the photoresist in the developer, and thus accelerate the edge etching to reduce the linewidth (Table 3). The SEM cross-section of Recipe 3 after 30 mJ exposure showed that the undercut could be maintained at a small level (Figure 8b). Moreover, the relationship between film thickness and energy dose became stable after 30 mJ, which was similar to that of Recipe 2. The film thickness of Recipe 3 was slightly smaller than Recipe 2, which was speculated to be related to the higher amount of hydrophilic monomers. The hydrophilic monomers increased the solubility of the photoresist, leading to a more significant loss of film thickness during alkaline development. However, due to the reactivity enhancement of Recipe 3, the polymerization was sufficient enough at 30 mJ, resulting in only a small thickness loss compared to Recipe 2. Therefore, an intact pattern, stable thickness and proper linewidth could be achieved by Recipe 3 at the energy dose of 30 mJ.

Table 3. Linewidth of Recipe 1, 2 and 3 after the post-baking process.

Photoresist	Recipe 1	Recipe 2	Recipe 3
Target linewidth (μm)		103±0.5	
Practical linewidth (μm)	103.38	108.60	103.46

Finally, a comprehensive process and optical performance evaluation was conducted on Recipe 3. As shown in the Figure 10, at an exposure energy of 30 mJ, a complete pattern with a minimum line width of 10 μm was achieved. The color coordinates on the CIE 1931 chromaticity diagram closely overlap with the standard sRGB color points [12, 13]. This implies that we have developed a red photoresist capable of meeting over 99% of the sRGB color space with a resolution of 10 μm, suitable for conventional TV screens, displays, laptops, and other similar products. In comparison to commonly used commercial red photoresists with a sensitivity of 40 mJ, formulation 3 achieves a 25% reduction in exposure time under the same exposure light source. This improvement directly translates to increased productivity and economic benefits for panel manufacturers.

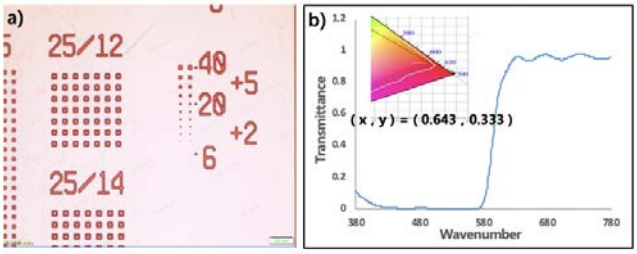

Figure 10. Properties of the red CPR based on Recipe 3: (a) Photolithographic resolution and (b) transmittance spectra of the red CF and its corresponding chromaticity @ CIE 1931.

4. Summary

Starting with the peeling of the red photoresist at an exposure dose of 30 mJ, the mechanism of pattern peeling was studied and the pivotal factor affecting the pattern peeling was discovered, which was closely related to the depth of undercut after development. By increasing the proportion of the photocuring components in the recipe, including increasing the ratio of the photoinitiator and monomers/resin, the reactivity of new photoresists could be improved. Meanwhile, increasing the proportion of hydrophilic monomer, DPEA-12, could effectively maintain the balance between the photocuring, development and linewidth. The new recipe could control the undercut within 1 μm after development and overcome the peeling problem during manufacturing. Finally, we achieved the optimal recipe for balanced optics and processes with the lowest photosensitivity of 30 mJ in the TFT-LCD panel industry.

5. Acknowledgments

This work is financially supported by the National Key R&D Program of China (2023YFB3608901), the National Natural Science Foundation of China (Grant No. 62205058), the

Guangdong Basic and Applied Basic Research Foundation (No. 2021A1515110085), the Shenzhen Fundamental Research Program (No. GXWD20201231165807007-202008101-13811001), the Development and Reform Commission of Shenzhen Municipality (XMHT20220106002), and the Shenzhen Science and Technology Program (JSGG20220831103402005).

The authors declare that they have no known competing financial interests or personal relationships that could have appeared to influence the work reported in this paper.

6. Reference

[1] Chen KS, Wang CH, Chen HT. A MAIC approach to TFT-LCD panel quality improvement. Microelectronics Reliability. 2006;46(7):1189-98.

[2] Huang CY, Lu HH, Ieee. Evaluating Key Factors for Selecting Capital Equipment Suppliers A Study of Small and Medium-Sized TFT-LCD Manufacturers. Proc International Conference on Applied System Innovation (IEEE ICASI). Fuzhou Univ, Okinawa, JAPAN2016.

[3] Jang YJ, Choi GH, Ieee. Introduction to automated material handling systems in LCD panel production lines. Proc IEEE International Conference on Automation Science and Engineering. Shanghai, PEOPLES R CHINA2006. p. 223-+.

[4] Park S, Park J, Lee S, Park J. New Dyes Based on Anthraquinone Derivatives for Color Filter Colorants. Journal of Nanoscience and Nanotechnology. 2014;14(8):6435-7.

[5] Tsuda，K. 1993_Displays_Colour filters for LCDs. Displays. 1993;115-124(14).

[6] Fu JM, Li Y, Guo JL, Gao HJ. Pigment-dispersed resists for color filters. Proc Conference on Display Devices and Systems II. Beijing, Peoples R China1998. p. 116-21.

[7] Lee RJ, Fan C, Cheng TS, Wu JL. Pigment-dispersed color resist with high resolution for advanced color filter application. Proc 5th Asian Symposium on Information Display (ASID 99). Natl Chiao Tung Univ, Hsinchu, Taiwan1999. p. 359-63.

[8] Pan Z. Polymer Chemistry (Enhanced Edition, 1st). Chemical Industry Press, Beijing 2007.

[9] Huang TY, Cheng WT. The Effect of Photo-initiator on the Contrast Curve of Negative-work Photo-resist. Journal of Photopolymer Science and Technology. 2011;24(6):643-6.

[10] Dietliker K, Jung TJ, Benkhoff J, Kura H, Matsumoto A, Oka H, et al. New developments in photoinitiators. Macromolecular Symposia. 2004;217:77-97.

[11] Sameshima K, Kura H, Matsuoka Y, Sotome H, Miyasaka H. Improvement of the photopolymerization and bottom-curing performance of benzocarbazole oxime ester photoinitiators with red-shifted absorption. Japanese Journal of Applied Physics. 2022;61(3).

[12] Kim ES, Kim DJ, Lee SI. Chromatic Error Correction Using sRGB Color Space. Journal of Nanoelectronics and Optoelectronics. 2016;11(2):239-43.

[13] Rehák R, Bodrogi P, Schanda J. On the use of the sRGB colour space. Displays. 1999;20(4):165-70.